Performance Analysis of Big Model Transmission under Double Rayleigh Fading

Ying Sun[1,*], Jiajia Huang[1], and Fusheng Wei[1]

[1]Guangdong Power Grid Co., Ltd, Guangzhou, China.

Abstract

The recent big model such as GPT-3.5 possesses an extensive understanding of natural language, and it can perform a wide range of tasks, making it a significant advancement in the field of artificial intelligence (AI). A critical challenge in the design and implementation of big model is that it imposes a heavy load on the wireless transmission due to a huge size of the deep network parameters, especially for the distributed implementation. To tackle this challenge, we investigate big model transmission under practical double Rayleigh fading environments, where the big model is simultaneously distributed to multiple training nodes through wireless transmission. To evaluate the system performance, we study the system outage probability (OP) based on the transmission latency, where an analytical expression is derived for the OP, which is used to evaluate the performance of big model transmission under double Rayleigh fading environments. Finally, we present some simulations under double Rayleigh fading environments, in order to show the validity of the proposed big model transmission.

1. Introduction

The development of big model represents a fascinating journey through the evolution of neural networks, marked by significant milestones in the field of artificial intelligence [1–3]. It began with the inception of neural networks, where early attempts to simulate the human brain's interconnected neurons laid the foundation. However, it was the advent of deep neural networks that truly revolutionized the landscape [4–6]. With the introduction of deep learning, multiple layers of interconnected neurons enabled the extraction of intricate features from complex data, paving the way for more accurate and powerful models [7–9]. This progression led to the birth of big model, exemplified by giants like GPT-3.5. These models, with their massive scale and extensive understanding of natural language, represent the culmination of years of research and innovation in deep learning. As computational power, data availability, and algorithmic advancements grew, big model emerged as pivotal tools, capable of performing a wide range of tasks and driving significant advancements in the field of artificial intelligence [10–12]. Their development reflects the relentless pursuit of pushing the boundaries of AI, enabling applications that were once considered futuristic to become a reality [13–15].

Developing and deploying big model presents a cascade of challenges. These include acquiring the substantial computational resources required for training, curating high-quality and diverse datasets, enhancing generalization to new tasks through techniques like transfer learning, addressing interpretability for transparent decision-making, and ensuring energy efficiency during training and inference. Another challenge is achieving low-latency inference for real-time applications via model compression and hardware acceleration. Additionally, fortifying models against adversarial attacks and distribution shifts and navigating ethical considerations concerning fairness and privacy are important. Maintaining scalability as data and tasks grow is another hurdle. Ultimately, there's the pivotal challenge of devising efficient wireless transmission

---

*Corresponding author. Email: Sunying.eecs@hotmail.com.

strategies to distribute big model, particularly in distributed settings or resource-constrained environments, where managing the heavy network load imposed by the size of model parameters is a critical factor in realizing the practical utility of big model [16–18].

Efficiently transmitting data, especially for supporting big model, involves a multi-pronged approach. One approach is the leveraging model compression techniques, such as pruning, quantization, and knowledge distillation, which can help reduce the size of the model. One more approach is to utilize efficient compression algorithms, like Huffman coding or arithmetic coding, to minimize the size of the transmitted data. Another approach is to adopt adaptive transmission strategies that prioritize sending critical model components first and utilize error correction codes to ensure robustness against wireless channel errors. In this direction, leveraging distributed computing and edge processing can be used to offload computation and reduce the amount of data needing transmission. In addition, the wireless communication protocol can be optimized by considering factors such as channel conditions, data prioritization, and latency requirements. In further, some advanced techniques have been explored like federated learning to enable collaborative model updates without transmitting raw data, reducing bandwidth needs while maintaining model performance, thus collectively addressing the significant challenge of wireless transmission for big model [19–22].

Reducing transmission outage probability in wireless communication has been a focus of extensive research, with relay, caching, and edge computing techniques playing pivotal roles [23–25]. Cooperative communication, network coding, and relay selection strategies optimize relay-based data transmission, while caching techniques such as content-centric networking and proactive caching reduce content retrieval delays. Edge computing paradigms like Mobile Edge Computing (MEC) and fog computing bring computation closer to the network edge, diminishing latency and enhancing reliability [26–28]. These techniques, coupled with advances in massive MIMO and coding-based caching, are collectively contributing to more robust and efficient wireless networks, addressing the critical challenge of minimizing transmission outage probability in modern communications.

In order to facilitate the advancement of big model, we undertake a comprehensive investigation into the transmission challenges they face within realistic double Rayleigh fading environments, where the big model needs to be efficiently distributed across multiple training nodes. Our focus extends to evaluate the overall system performance, specifically honing in on the critical metric of system outage probability (OP). This performance assessment hinges on the transmission latency, a pivotal factor in real-world deployments of big model.
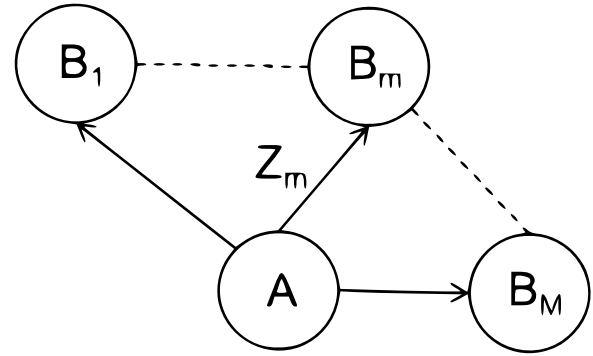
Figure 1. System model of big model transmission with multiple training nodes under double Rayleigh fading channels.

We delve deep into this metric, leveraging our findings to derive a precise analytical expression that quantifies the outage probability. To affirm the robustness and efficacy of our proposed big model transmission strategy, we meticulously execute a series of simulations conducted under the demanding conditions of double Rayleigh fading environments. Through these simulations, we aim to showcase the practical validity and effectiveness of our proposed approach, elucidating its potential to overcome the challenges posed by wireless transmission, especially in distributed settings, which are pivotal for the successful deployment of big model across a spectrum of applications.

2. SYSTEM MODEL of Big model transmission

As shown in Fig. 1, we study the system model of big model transmission with multiple training nodes under double Rayleigh fading channels [29–32], which includes one sender A, and M receivers $\{B_m \mid 1 \in m \in M\}$. Moreover, A has a heavy task of big model parameter that needs to be sent to M training nodes uniformly and simultaneously. Specifically, the wireless channel parameter between A and B_m, denoted as z_m, could be represented as

$$z_m = g_{1,m} \cdot g_{2,m}, \tag{1}$$

where $g_{1,m}$ and $g_{2,m}$ are the first-hop double Rayleigh fading channel parameter and second-hop double Rayleigh fading channel parameter, respectively. Moreover, the parameters $g_{1,m}$ and $g_{2,m}$ can be modeled as

$$g_{1,m} \sim \mathcal{CN}(0, \xi_1), \tag{2}$$
$$g_{2,m} \sim \mathcal{CN}(0, \xi_2), \tag{3}$$

where ξ_1 and ξ_2 are the average channel gain of the first-hop and second-hop for the double Rayleigh fading channels. Thus, the available transmission rate between A and B_m is

$$R_m = W \log_2\left(1 + \frac{P}{\sigma^2}|z_m|^2\right), \tag{4}$$

where W is the allocated bandwidth of the link A-B_m, P is the transmit power of A, and σ^2 is the variance of additive white Gaussian noise (AWGN). In this network, the node A has the task of K bits, that needs to be sent to M training nodes uniformly and simultaneously. Hence, the transmission latency from A to the training node B_m is

$$t_m = \frac{\tilde{k}}{R_m}, \tag{5}$$

where $\tilde{k} = \frac{K}{M}$ is denoted by the task length allocated to each training node.

3. PERFORMANCE ANALYSIS of big model transmission

In this section, we give a definition of the system outage probability for the big model transmission, and then derive the associated closed-form expression for the outage probability. In particular, the system outage occurs when at least one transmission latency between the sender A to the M training nodes is larger than a given latency threshold γ_{th},

$$P_{out} = 1 - \Pr\left(t_1 < \gamma_{th}, t_2 < \gamma_{th}, \cdots, t_M < \gamma_{th}\right), \tag{6}$$

$$= 1 - \Pr\left(t_1 < \gamma_{th}\right) \cdot \Pr(t_2 < \gamma_{th}) \cdots \Pr(t_M < \gamma_{th}), \tag{7}$$

$$= 1 - \left[\Pr\left(t_1 < \gamma_{th}\right)\right]^M. \tag{8}$$

Since the transmission latencies $\{t_1, t_2, \ldots, t_M\}$ are independently and identically distributed, we can simplify the above probability of the system outage to solve for the probability that the transmission latency between the training node B_m and A satisfies the latency threshold, i.e.,

$$P_m = 1 - \Pr(t_m < \gamma_{th}), \tag{9}$$

$$= 1 - \Pr\left(\frac{\tilde{k}}{W \log_2\left(1 + \frac{P}{\sigma^2}|z_m|^2\right)} < \gamma_{th}\right), \tag{10}$$

$$= \Pr\left(|z_m|^2 > \left(2^{\frac{\tilde{k}}{W\gamma_{th}}} - 1\right)\frac{\sigma^2}{P}\right). \tag{11}$$

Secondly, we derive the associated closed-form expression for the outage probability. In the first, because of

$$g_{1m} \sim CN(0, \xi_1), \tag{12}$$

$$g_{2m} \sim CN(0, \xi_2), \tag{13}$$

$$z_m = g_{1,m} \cdot g_{2,m}, \tag{14}$$

we can simplify the above notations as,

$$|g_{1m}|^2 = X, \qquad |g_{2m}|^2 = Y, \tag{15}$$

and then we have,

$$P_m = 1 - \Pr\left[|z_m|^2 \le (2^{\frac{\tilde{k}}{W\gamma_{th}}} - 1)\frac{\sigma^2}{P}\right], \tag{16}$$

$$= 1 - \Pr\left[|g_{1m}|^2 \le \frac{(2^{\frac{\tilde{k}}{W\gamma_{th}}} - 1)\frac{\sigma^2}{P}}{|g_{2m}|^2}\right], \tag{17}$$

$$= 1 - \int_0^\infty \int_0^{\frac{(2^{\frac{\tilde{k}}{W\gamma_{th}}} - 1)\frac{\sigma^2}{P}}{Y}} f_{X,Y}(x,y)\,dx\,dy. \tag{18}$$

We can further write P_m as,

$$P_m = 1 - \int_0^\infty \int_0^{\frac{(2^{\frac{\tilde{k}}{W\gamma_{th}}} - 1)\sigma^2}{Py}} \frac{1}{\xi_1}e^{-\frac{x}{\xi_1}}\frac{1}{\xi_2}e^{-\frac{y}{\xi_2}}\,dx\,dy, \tag{19}$$

$$= 1 - \int_0^\infty \frac{1}{\xi_1}e^{-\frac{x}{\xi_1}}\frac{1}{\xi_2}e^{-\frac{y}{\xi_2}}\Big|_{\substack{x=0 \\ x=\frac{(2^{\frac{\tilde{k}}{W\gamma_{th}}} - 1)\sigma^2}{Py}}}\,dy, \tag{20}$$

$$= 1 - \int_0^\infty \frac{1}{\xi_2}e^{-\frac{y}{\xi_2}} - \frac{1}{\xi_2}e^{-\frac{y}{\xi_2}}e^{-\frac{(2^{\frac{\tilde{k}}{W\gamma_{th}}} - 1)\sigma^2}{Py\xi_1}}\,dy. \tag{21}$$

By solving the above integral, we can write P_m in further as

$$P_m = 1 - \left[e^{-\frac{y}{\xi_2}}\Big|_\infty^0 - \int_0^\infty \frac{1}{\xi_2}e^{-\frac{y}{\xi_2}}e^{-\frac{(2^{\frac{\tilde{k}}{W\gamma_{th}}} - 1)\sigma^2}{Py\xi_1}}\,dy\right], \tag{22}$$

$$= \int_0^\infty \frac{1}{\xi_2}e^{-\frac{y}{\xi_2}}e^{-\frac{(2^{\frac{\tilde{k}}{W\gamma_{th}}} - 1)\sigma^2}{Py\xi_1}}\,dy. \tag{23}$$

We can further have,

$$P_m = \frac{1}{\xi_2}\sqrt{\frac{4(2^{\frac{\tilde{k}}{W\gamma_{th}}} - 1)\sigma^2\xi_2}{P\xi_1}}K_1\left(\sqrt{\frac{4(2^{\frac{\tilde{k}}{W\gamma_{th}}} - 1)\sigma^2}{P\xi_1\xi_2}}\right), \tag{24}$$

$$= 2\sigma\sqrt{\frac{2^{\frac{\tilde{k}}{W\gamma_{th}}} - 1}{P\xi_1\xi_2}}K_1\left(2\sigma\sqrt{\frac{2^{\frac{\tilde{k}}{W\gamma_{th}}} - 1}{P\xi_1\xi_2}}\right), \tag{25}$$

where $K_1(x)$ denotes the first-order modified Bessel function of the second kind [33].

Finally, the outage probability of the big model transmission is given by

$$P_{out} = 1 - (P_m)^M, \tag{26}$$

$$= 1 - \left[2\sigma\sqrt{\frac{2^{\frac{\tilde{k}}{W\gamma_{th}}} - 1}{P\xi_1\xi_2}}K_1\left(2\sigma\sqrt{\frac{2^{\frac{\tilde{k}}{W\gamma_{th}}} - 1}{P\xi_1\xi_2}}\right)\right]^M. \tag{27}$$

From the above analytical expression of P_{out}, we can readily evaluate the failure probability of big model transmission, under double Rayleigh fading environments.
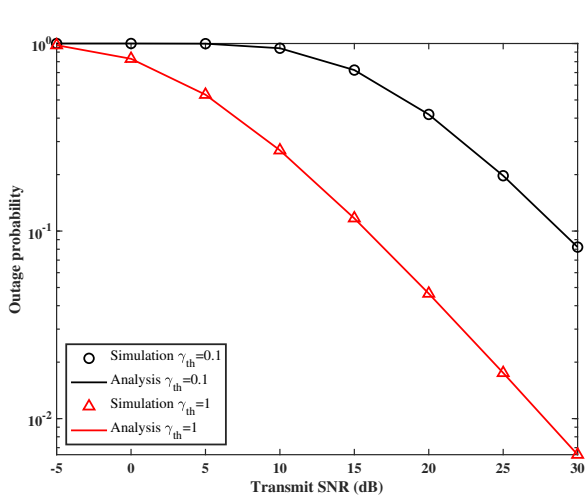
Figure 2. Outage probability of big model transmission versus the transmit SNR.

Figure 3. Outage probability of big model transmission versus K.

4. SIMULATION RESULTS AND DISCUSSIONS for big model transmission

In this section, we present a series of simulations designed to empirically validate the analytical findings on the big model transmission. If not specified, the parameters of big model transmission are set as follows. Firstly, the task length of the big model is $K = 1$MBits, while the communication bandwidth is $W = 1$MHz [34–36]. Secondly, the average channel gains ξ_1 and ξ_2 are both set to unity [37–39]. The transmit signal-to-noise ratio (SNR) is established at 10 dB, and the variance of AWGN is $\sigma^2 = 1$. Finally, the number of training nodes M is fixed to 5, and the latency threshold is $\gamma_{th} = 1$s.

Fig. 2 and Table 1 show the simulation and analysis results of the big model transmission versus the transmit SNR, where the SNR increases from -5 dB to 30 dB. From Fig. 2 and Table 1, it can be observed that the outage probability decreases with increasing SNR, which is due to a larger SNR leading to a higher transmission rate, which reduces the task transmission latency and eventually the outage probability. In addition, the analytical results overlap with the simulation ones, which validates the closed-form solution. For example, the simulated OP with SNR=25dB and $\gamma_{th} = 0.1$ is about 0.19724, while the associated analytical OP is about 0.19726. The simulated OP with SNR=25dB and $\gamma_{th} = 1$ is about 0.01752, while the associated analytical OP is about 0.01753. Finally, the outage probability with $\gamma = 0.1$ is consistently higher than that with $\gamma_{th} = 1$, indicating that a relaxed latency constraint can help reduce the communication outage probability.

Fig. 3 and Table 2 depict the impact of the task length K, on both analytical and simulated outage probabilities of the big model transmission. The value
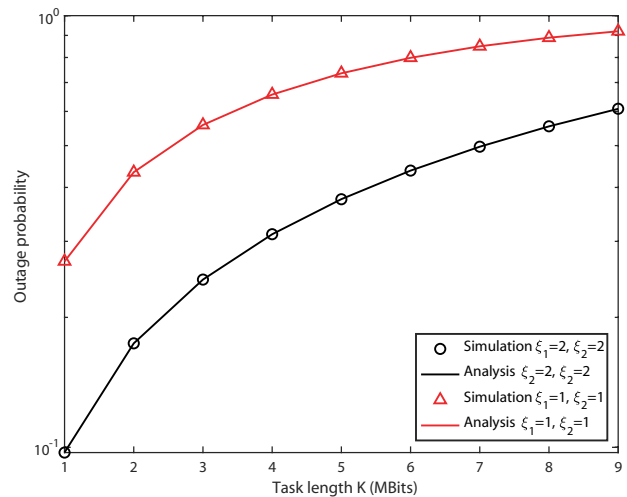
of K varies from 1 MBits to 9MBits, while ξ_1 and ξ_2 take values from the set of $\{1, 2\}$. In Fig. 3 and Table 2, it becomes evident that as the value of K increases, the outage probability also increases. This trend indicates that a higher value of K leads to a worse outage performance. Moreover, the overlap between the analytical and simulation results in Fig. 3 affirms the accuracy and validity of the derived expression for the outage probability. In particular, the simulated OP with $K = 1$Mbits and $\xi_1 = \xi_2 = 2$ is about 0.09724, while the associated analytical OP is about 0.09733. The simulated OP with $K = 1$Mbits and $\xi_1 = \xi_2 = 1$ is about 0.26963, while the associated analytical OP is about 0.26954. Additionally, the outage performance with $\xi_1 = 2$ and $\xi_2 = 2$ is notably superior to that with $\xi_1 = 1$ and $\xi_2 = 1$. This phenomenon appears from the fact that an increased value of ξ correlates with improved channel quality.

Fig. 4 and Table 3 show the effect of communication bandwidth W on the analyzed and simulated outage probability of the big model transmission, where W varies from 1MHz to 9MHz. As shown in Fig. 4 and Table 3, we can see that the outage probability shows a decreasing trend with the increase of W, which indicates that a larger communication bandwidth effectively reduces the outage probability, and the analyzed results overlap with the simulated results, which verifies the closed-form solution. For example, the simulated OP with $W = 9$MHz and $\gamma_{th} = 0.1$ is about 0.290482, while the associated analytical OP is about 0.290672. The simulated OP with $W = 9$MHz and $\gamma_{th} = 1$ is about 0.048064, while the associated analytical OP is about 0.048095. Moreover, the outage probability with $\gamma_{th} = 0.1$ is always higher than that with $\gamma_{th} = 1$, which is because that a higher

Table 1: Numerical outage probability of big model transmission versus the transmit SNR.

SNR (dB)	-5	0	5	10	15	20	25	30
sim: $\gamma_{th} = 0.1$	1.0000	0.9999	0.9979	0.9436	0.7217	0.4187	0.1972	0.0821
ana: $\gamma_{th} = 0.1$	1.0000	0.9999	0.9979	0.9437	0.7218	0.4185	0.1973	0.0821
sim: $\gamma_{th} = 1$	0.9796	0.8289	0.5333	0.2695	0.1170	0.0464	0.0175	0.0064
ana: $\gamma_{th} = 1$	0.9796	0.8289	0.5334	0.2696	0.1169	0.0464	0.0175	0.0064

Table 2: Numerical outage probability of big model transmission versus K.

K (Mbits)	1	2	3	4	5	6	7	8	9
sim: $\xi_{1,2} = 2$	0.0972	0.1741	0.2447	0.3117	0.3756	0.4376	0.4970	0.5542	0.6086
ana: $\xi_{1,2} = 2$	0.0973	0.1741	0.2447	0.3116	0.3758	0.4376	0.4970	0.5540	0.6084
sim: $\xi_{1,2} = 1$	0.2696	0.4336	0.5581	0.6566	0.7354	0.7988	0.8491	0.8889	0.9201
ana: $\xi_{1,2} = 1$	0.2696	0.4339	0.5582	0.6565	0.7353	0.7986	0.8491	0.8890	0.9200

Table 3: Numerical outage probability of big model transmission versus W.

W (MHz)	1	2	3	4	5	6	7	8	9
sim: $\gamma_{th} = 0.1$	0.9436	0.7353	0.5934	0.4999	0.4337	0.3847	0.3465	0.3157	0.2905
ana: $\gamma_{th} = 0.1$	0.9437	0.7353	0.5934	0.4999	0.4339	0.3847	0.3465	0.3158	0.2907
sim: $\gamma_{th} = 1$	0.2696	0.1609	0.1173	0.0934	0.0781	0.0673	0.0593	0.0531	0.0481
ana: $\gamma_{th} = 1$	0.2696	0.1609	0.1174	0.0934	0.0780	0.0672	0.0592	0.0530	0.0481

Table 4: Numerical outage probability of big model transmission versus M.

M	1	2	3	4	5	6	7	8	9	10
sim: $\xi_{1,2} = 2$	0.0901	0.0900	0.0926	0.0951	0.0974	0.0993	0.1012	0.1027	0.1041	0.1056
ana: $\xi_{1,2} = 2$	0.0899	0.0900	0.0926	0.0951	0.0973	0.0993	0.1011	0.1027	0.1041	0.1054
sim: $\xi_{1,2} = 1$	0.2334	0.2422	0.2528	0.2618	0.2701	0.2762	0.2818	0.2870	0.2920	0.2955
ana: $\xi_{1,2} = 1$	0.2334	0.2421	0.2528	0.2619	0.2696	0.2762	0.2820	0.2872	0.2918	0.2960

latency threshold can effectively improve the outage performance.

Fig. 5 and Table 4 illustrate the influence of the number of training nodes M, on both analytical and simulated outage probabilities of the big model transmission, where M varies within the range of 1 to 10, while parameters ξ_1 and ξ_2 assume values from the set {1, 2}. From the observation of Fig. 5 and Table 4, it becomes evident that an increase in the value of M leads to a corresponding increase in the outage probability. This observation shows that a higher M is associated with a deteriorating outage performance. Moreover, it is worth noting that the outage performance exhibits noticeable improvement when considering $\xi_1 = 2$ and $\xi_2 = 2$, in contrast to the scenario with $\xi_1 = 1$ and $\xi_2 = 1$. This gap can be attributed to the inherent correlation between the larger values of ξ and enhanced channel quality. It is essential to highlight that the alignment between the analytical and simulation results depicted in Fig. 5 substantiates the accuracy and validity of the derived analytical expression governing the outage probability.

5. conclusion

In conclusion, this paper addressed a critical challenge in the field of artificial intelligence, specifically related to the transmission of large models like GPT-3.5 in practical double Rayleigh fading environments. The
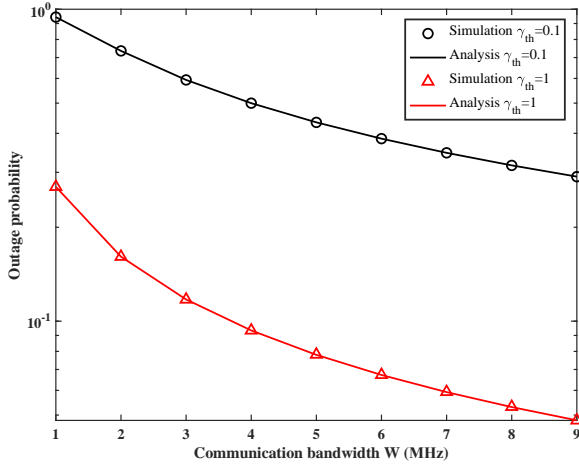
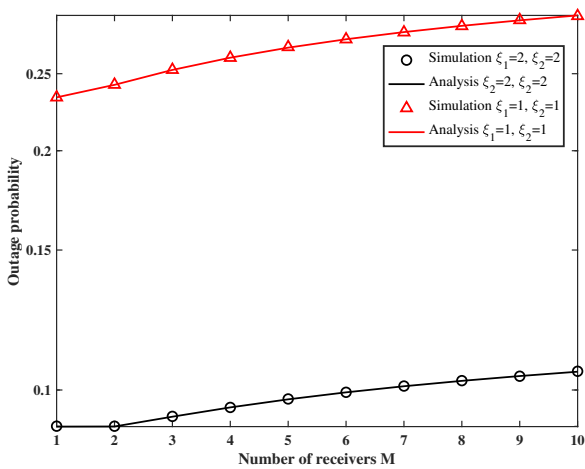**Figure 4.** Outage probability of big model transmission versus W.

Figure 5. Outage probability of big model transmission versus M.

study focused on distributed implementations, which were found to impose heavy loads on wireless transmission due to the massive size of network parameters. The investigation of system outage probability based on transmission latency provided valuable insights, and the derived analytical expression offered a framework for understanding the performance of big model transmission. The presented simulations validated the proposed approach and offered promising strategies for

handling the transmission challenges associated with the advanced AI models.

5.1. Copyright

References

[1] D. Chandra, P. Botsinis, D. Alanis, Z. Babar, S. X. Ng, and L. Hanzo, "On the road to quantum communications," *Infocommunications Journal*, vol. 14, no. 3, pp. 2–8, 2022.

[2] Z. Huang, L. Bai, X. Cheng, X. Yin, P. E. Mogensen, and X. Cai, "A non-stationary 6g V2V channel model with continuously arbitrary trajectory," *IEEE Trans. Veh. Technol.*, vol. 72, no. 1, pp. 4–19, 2023.

[3] A. E. Haddad and L. Najafizadeh, "The discriminative discrete basis problem: Definitions, algorithms, benchmarking, and application to brain's functional dynamics," *IEEE Trans. Signal Process.*, vol. 71, pp. 1–16, 2023.

[4] S. S. Mahdi and A. A. Abdullah, "Enhanced security of software-defined network and network slice through hybrid quantum key distribution protocol," *Infocommunications Journal*, 2022.

[5] Z. Xie, W. Chen, and H. V. Poor, "A unified framework for pushing in two-tier heterogeneous networks with mmwave hotspots," *IEEE Trans. Wirel. Commun.*, vol. 22, no. 1, pp. 19–31, 2023.

[6] Y. Fang, "-ary distributed arithmetic coding for uniform -ary sources," *IEEE Trans. Inf. Theory*, vol. 69, no. 1, pp. 47–74, 2023.

[7] T. Häckel, P. Meyer, F. Korf, and T. C. Schmidt, "Secure time-sensitive software-defined networking in vehicles," *IEEE Trans. Veh. Technol.*, vol. 72, no. 1, pp. 35–51, 2023.

[8] Y. Song, Z. Gong, Y. Chen, and C. Li, "Tensor-based sparse bayesian learning with intra-dimension correlation," *IEEE Trans. Signal Process.*, vol. 71, pp. 31–46, 2023.

[9] H. Wan and A. Nosratinia, "Short-block length polar-coded modulation for the relay channel," *IEEE Trans. Commun.*, vol. 71, no. 1, pp. 26–39, 2023.

[10] Q. Lu, S. Li, B. Bai, and J. Yuan, "Spatially-coupled faster-than-nyquist signaling: A joint solution to detection and code design," *IEEE Trans. Commun.*, vol. 71, no. 1, pp. 52–66, 2023.

[11] B. Han, V. Sciancalepore, Y. Xu, D. Feng, and H. D. Schotten, "Impatient queuing for intelligent task offloading in multiaccess edge computing," *IEEE Trans. Wirel. Commun.*, vol. 22, no. 1, pp. 59–72, 2023.

[12] H. Hou, Y. S. Han, P. P. C. Lee, Y. Wu, G. Han, and M. Blaum, "A generalization of array codes with local properties and efficient encoding/decoding," *IEEE Trans. Inf. Theory*, vol. 69, no. 1, pp. 107–125, 2023.

[13] Y. Xiong, S. Sun, L. Liu, Z. Zhang, and N. Wei, "Performance analysis and bit allocation of cell-free massive MIMO network with variable-resolution adcs," *IEEE Trans. Commun.*, vol. 71, no. 1, pp. 67–82, 2023.

[14] J. Shao, Y. Mao, and J. Zhang, "Task-oriented communication for multidevice cooperative edge inference," *IEEE Trans. Wirel. Commun.*, vol. 22, no. 1, pp. 73–87, 2023.

[15] H. H. López and G. L. Matthews, "Multivariate goppa codes," *IEEE Trans. Inf. Theory*, vol. 69, no. 1, pp. 126–137, 2023.

[16] Y. Sun, D. Wu, X. S. Fang, and J. Ren, "On-glass grid structure and its application in highly-transparent antenna for internet of vehicles," *IEEE Trans. Veh. Technol.*, vol. 72, no. 1, pp. 93–101, 2023.

[17] P. Tichavský, O. Straka, and J. Duník, "Grid-based bayesian filters with functional decomposition of transient density," *IEEE Trans. Signal Process.*, vol. 71, pp. 92–104, 2023.

[18] C. Zeng, J. Wang, C. Ding, M. Lin, and J. Wang, "MIMO unmanned surface vessels enabled maritime wireless network coexisting with satellite network: Beamforming and trajectory design," *IEEE Trans. Commun.*, vol. 71, no. 1, pp. 83–100, 2023.

[19] Q. Li, R. Gan, J. Liang, and S. J. Godsill, "An adaptive and scalable multi-object tracker based on the non-homogeneous poisson process," *IEEE Trans. Signal Process.*, vol. 71, pp. 105–120, 2023.

[20] F. Hu, Y. Deng, and A. H. Aghvami, "Scalable multi-agent reinforcement learning for dynamic coordinated multipoint clustering," *IEEE Trans. Commun.*, vol. 71, no. 1, pp. 101–114, 2023.

[21] H. Hui and W. Chen, "Joint scheduling of proactive pushing and on-demand transmission over shared spectrum for profit maximization," *IEEE Trans. Wirel. Commun.*, vol. 22, no. 1, pp. 107–121, 2023.

[22] W. Yu, Y. Xi, X. Wei, and G. Ge, "Balanced set codes with small intersections," *IEEE Trans. Inf. Theory*, vol. 69, no. 1, pp. 147–156, 2023.

[23] J. Sun, J. Yang, G. Gui, and H. Sari, "In-motion alignment method of SINS under the geographic latitude uncertainty," *IEEE Trans. Veh. Technol.*, vol. 72, no. 1, pp. 125–135, 2023.

[24] Z. Zhang, Z. Shi, and Y. Gu, "Ziv-zakai bound for doas estimation," *IEEE Trans. Signal Process.*, vol. 71, pp. 136–149, 2023.

[25] S. Guo and X. Zhao, "Multi-agent deep reinforcement learning based transmission latency minimization for delay-sensitive cognitive satellite-uav networks," *IEEE Trans. Commun.*, vol. 71, no. 1, pp. 131–144, 2023.

[26] X. Fang, W. Feng, Y. Wang, Y. Chen, N. Ge, Z. Ding, and H. Zhu, "Noma-based hybrid satellite-uav-terrestrial networks for 6g maritime coverage," *IEEE Trans. Wirel. Commun.*, vol. 22, no. 1, pp. 138–152, 2023.

[27] R. Gabrys, V. Guruswami, J. L. Ribeiro, and K. Wu, "Beyond single-deletion correcting codes: Substitutions and transpositions," *IEEE Trans. Inf. Theory*, vol. 69,

no. 1, pp. 169–186, 2023.

[28] E.-s. Azougaghe, A. Farchane, S. Safi, and M. Belkasmi, "Turbo decoding of concatenated codes based on rs codes using adapted scaling factors," *Infocommunications Journal*, vol. 14, no. 1, pp. 11–16, 2022.

[29] Y. Liu, Z. Tan, A. W. H. Khong, and H. Liu, "An iterative implementation-based approach for joint source localization and association under multipath propagation environments," *IEEE Trans. Signal Process.*, vol. 71, pp. 121–135, 2023.

[30] K. Ma, S. Du, H. Zou, W. Tian, Z. Wang, and S. Chen, "Deep learning assisted mmwave beam prediction for heterogeneous networks: A dual-band fusion approach," *IEEE Trans. Commun.*, vol. 71, no. 1, pp. 115–130, 2023.

[31] B. Banerjee, R. C. Elliott, W. A. Krzymien, and H. Farmanbar, "Downlink channel estimation for FDD massive MIMO using conditional generative adversarial networks," *IEEE Trans. Wirel. Commun.*, vol. 22, no. 1, pp. 122–137, 2023.

[32] S. Liu and L. Ji, "Double multilevel constructions for constant dimension codes," *IEEE Trans. Inf. Theory*, vol. 69, no. 1, pp. 157–168, 2023.

[33] I. S. Gradshteyn and I. M. Ryzhik, *Table of Integrals, Series, and Products*, 7th ed. San Diego, CA: Academic, 2007.

[34] X. Chen, W. Wei, Q. Yan, N. Yang, and J. Huang, "Time-delay deep q-network based retarder torque tracking control framework for heavy-duty vehicles," *IEEE Trans. Veh. Technol.*, vol. 72, no. 1, pp. 149–161, 2023.

[35] Z. Yang, F. Li, and D. Zhang, "A joint model extraction and data detection framework for IRS-NOMA system," *IEEE Trans. Signal Process.*, vol. 71, pp. 164–177, 2023.

[36] T. Zhang, K. Zhu, S. Zheng, D. Niyato, and N. C. Luong, "Trajectory design and power control for joint radar and communication enabled multi-uav cooperative detection systems," *IEEE Trans. Commun.*, vol. 71, no. 1, pp. 158–172, 2023.

[37] M. Zaher, Ö. T. Demir, E. Björnson, and M. Petrova, "Learning-based downlink power allocation in cell-free massive MIMO systems," *IEEE Trans. Wirel. Commun.*, vol. 22, no. 1, pp. 174–188, 2023.

[38] M. Salman and M. K. Varanasi, "The -user DM broadcast channel with two groupcast messages: Achievable rate regions and the combination network as a case study," *IEEE Trans. Inf. Theory*, vol. 69, no. 1, pp. 194–222, 2023.

[39] H. Farran, D. Khoury, and L. Bokor, "A comprehensive survey on the application of blockchain/hash chain technologies in v2x communications," *Infocommunications Journal*, vol. 14, no. 1, pp. 24–35, 2022.